Supporting Information

Uglietti et al. 10.1073/pnas.1421119112

SI Text

Potential Source Area Dust. Trace element composition was determined in two dust samples collected in plastic containers, ~500 m west of the Quelccaya ice cap (Dataset S2), as this is the most likely potential source area of aeolian dust entrapped in the Quelccaya North Dome Ice Core (QND). To evaluate its trace element composition, we added a few grams of dust to 1 L of ultrapure water and separated the "aeolian-like" fraction by gravitational settling (1, 2). The supernatant solution was sampled with a pipette after 2 min. An aliquot was immediately analyzed with a Beckman–Coulter Multisizer 4. Dust size modes were <10 μm, i.e., within the range of dust sizes entrapped in QND. Another supernatant aliquot was transferred with a pipette to a 15-mL low-density polyethylene bottle (Nalgene), acidified with 2% (vol/vol) HNO_3 and analyzed after 30 d by ICP-SFMS with the same methodology used to analyze the QND ice samples (3).

The A.D. 1600 Huaynaputina Ash Fingerprint. Around the A.D. 1600 horizon, QND contains ejecta from the well-documented eruption of Huaynaputina, a volcano, which is located ~300 km south of the Quelccaya ice cap. Tephra from the A.D. 1600 Huaynaputina eruption have been observed in another ice core from Quelccaya (4), and trace element data also provide evidence of the ash fallout. In fact, notable increases in the concentration of most trace elements occur around A.D. 1600 in the ice core record (Fig. 2 and Figs. S2 and S3). The impact of the Huaynaputina tephra on trace elements appears to have lasted ~10 y, probably due to secondary transport from successive deflation of Huaynaputina ash initially deposited on the deglaciated margins of the ice cap.

We have determined the trace element composition in the Huaynaputina QND tephra layer and in Huaynaputina ash collected at the archaeological site of Cerro Trapiche (17°11'S, 70°58'W; near Moquega, Peru) (Dataset S2). Trace element composition of Huaynaputina ash was determined by ICP-SFMS using our methodology for investigating dust from potential source areas (see Potential Source Area Dust section). Comparison of mass ratios confirms earlier findings (based on direct tephra observations and major elemental analysis) that Huaynaputina is the source of the tephra particles entrapped at this depth (4).

The similarity of the EFc values calculated in these tephra ice layers, taking as a reference the trace element compositions of Huaynaputina ash and dust collected at near the Quelccaya ice cap (Dataset S2), also indicates that the composition of Quelccaya local dust and Huaynaputina ash match rather well, probably as a consequence of the common andesite geological background at the two sites. This ultimately explains why the calculated EFc of the Huaynaputina tephra layer in QND ice does not show a positive anomaly (Fig. 2 and Figs. S2 and S3).

Trace Element Evidence of Volcanic Ash Horizons. We preliminarily searched for possible ash horizons in the QND layers by identifying anomalous single EFc values of typical volcanic elements such as Ag, Bi, Cd, Cr, Cu, Pb, Sb, and Tl. We define anomalous EFc values as peaks that are 3 times larger than the median during the relatively anthropogenically unperturbed A.D. 793–1450 time period and 5 times larger than the median during the A.D. 1450–1900, a period of persistent contribution of metallurgic origin. The A.D. 1900–1989 period was excluded from this analysis because of the much larger anthropogenic origin of most of the trace elements.

We tentatively compared the timing of the anomalous EFc values in QND with a recent compilation of volcanic events recorded in a composite Antarctic ice core record (5) (Dataset S3). Possible volcanic events occur within 1 y of the eruption of Krakatoa (A.D. 1883), coincident with Cosiguina (A.D. 1835), within 5 y of Tambora (A.D. 1815), within 25 y of Kuwae (A.D. 1453), and within 1 y of Samalas (A.D. 1257). The timing of several unknown eruptions reported in the Antarctic compilation (5), is potentially coincident with most of the EFc spikes in the deepest part of QND (before A.D. 1450), where, however, annual layers cannot be recognized and dating is more uncertain. Nevertheless, we note that after A.D. 1450, 10 out of 17 well-dated anomalous EFc values do not match with any volcanic event recorded in the Antarctic array, suggesting that both global and Andean volcanism played a significant but occasional role in determining the geochemistry of QND trace elements during precolonial and colonial time.

Ag Determinations in the Quelccaya North Dome Ice Core. Ag determinations need an important clarification because, while mining activities during the Hispanic vice-royal period were primarily concerned with Ag production, Ag levels in QND do not exhibit any remarkable increases over this time period. This could be due to: (*i*) the very low Ag concentrations ($pg \cdot g^{-1}$ level) that are magnified by the deposition of Ag as AgCl in ice core sample solutions (3); (*ii*) the higher uncertainty in the Ag determination; and (*iii*) the relatively high crustal and volcanic Ag background in the ice samples. It is possible, however, that Ag anthropogenic enrichment becomes apparent in the QND record at around A.D. 1700, but this remains uncertain (Fig. S2).

Because Ag cannot be very useful, Pb serves thus as the cornerstone of our interpretation. Pb was chosen for two reasons: First, Incan smelting technologies relied upon argentiferous galena [(Pb, Ag)S] as a flux during smelting (6), which led to excessive Pb volatilization. Second, depositions of Pb during the examined period are better known than for the other elements measured, as Pb has been quantified also in South American lake sediment cores and in ice cores from other high-latitude and high-altitude environments (7–13).

Statistical Analysis of Trace Element Concentrations. A Ward hierarchical analysis was applied to the matrix of the first three principal components (with a cumulative explained variance of nearly 90%), extracted from the ranked concentrations (2, 14), to study the association of the chemical variables (trace elements) during the entire period (A.D. 793–1989) and during the three subperiods studied in this work. The statistical analysis of the entire data set (Fig. S4*A*) confirms the crustal character for Al, Co, Fe, Mn, Rb, Ti, Tl, V, and U and suggests an overall significant nonlithogenic contribution for Ag, As, Bi, Cd, Cr, Cu, Mo, Pb, and Sb.

When peculiar time periods are considered, additional observations can be performed. During the pre-Inca part of the record (A.D. 793–1450) (Fig. S4*B*), the statistical analysis links Ag and Cd, suggesting that their presence may result from quiescent degassing volcanic emissions, while the grouping of Cu and Mo with Bi, Cr, Pb, and Sb may be evidence of the intermittent input from pre-Inca mining and metallurgic activities as noted in sediment cores recovered from lakes located near large polymetallic mines at Morococha (Peru) (8) and Potosí (Bolivia) (7). During the A.D. 1450–1900 period, the statistical analysis indicates a common metallurgic emission and depositional pattern for Ag, Bi, Cr, Cu, Mo, Pb, and Sb (Fig. S4*C*) while, during the A.D. 1900–1989 period, additional links emerge, for instance, for Mo and Sb or Cr and Cu, indicating an increase in the complexity of the sources of anthropogenic emissions at various spatial scales during the 20th century (Fig. S4*D*).

Seasonality of the Crustal Enrichment Factors. EFc values were assigned to wet and dry seasons (Fig. S6), which were distinguished by the relative seasonal concentrations of Fe taken as a proxy of mineral dust (assumed to be high during the dry season and low during the wet season). As a threshold to discriminate samples representing the dry and the wet season during each year, we used the average Fe concentration calculated within each year. In this way, it was possible to seasonally discriminate the data only during the A.D. 1495–1989 time period when there were at least two samples per year (Fig. S1).

1. Wegner A, et al. (2012) Change in dust variability in the Atlantic sector of Antarctica at the end of the last deglaciation. *Clim. Past* 8:135–147.
2. Gabrielli P, et al. (2014) Deglaciated areas of Kilimanjaro as a source of volcanic trace elements deposited on the ice cap during the late Holocene. *Quat Sci Rev* 93: 1–10.
3. Uglietti C, Gabrielli P, Olesik JW, Lutton A, Thompson LG (2014) Large variability of trace element mass fractions determined by ICP-SFMS in ice core samples from worldwide high altitude glaciers. *Appl Geochem* 47:109–121.
4. Thompson LG, Mosley-Thompson E, Dansgaard W, Grootes PM (1986) The little ice age as recorded in the stratigraphy of the tropical Quelccaya ice cap. *Science* 234(4774):361–364.
5. Sigl M, et al. (2014) Insights from Antarctica on volcanic forcing during the Common Era. *Nat Clim Change* 4(8):693–697.
6. Brown KW (2012) *A History of Mining in Latin America from the Colonial Era to the Present* (Univ of New Mexico Press, Albuquerque, NM).
7. Abbott MB, Wolfe AP (2003) Intensive pre-Incan metallurgy recorded by lake sediments from the Bolivian Andes. *Science* 301(5641):1893–1895.
8. Cooke CA, Abbott MB, Wolfe AP, Kittleson JL (2007) A millennium of metallurgy recorded by lake sediments from Morococha, Peruvian Andes. *Environ Sci Technol* 41(10):3469–3474.
9. Cooke CA, Wolfe AP, Hobbs WO (2009) Lake-sediment geochemistry reveals 1400 years of evolving extractive metallurgy at Cerro de Pasco, Peruvian Andes. *Geology* 37:1019–1022.
10. Lee K, et al. (2011) Isotopic signatures for natural versus anthropogenic Pb in high-altitude Mt. Everest ice cores during the past 800 years. *Sci Total Environ* 412-413(0):194–202.
11. McConnell JR, Lamorey GW, Hutterli MA (2002) A 250-year high-resolution record of Pb flux and crustal enrichment in central Greenland. *Geophys Res Lett* 29(23): 2130–2132.
12. McConnell JR, et al. (2014) Antarctic-wide array of high-resolution ice core records reveals pervasive lead pollution began in 1889 and persists today. *Sci Rep* 4:5848.
13. Schwikowski M, et al. (2004) Post-17th-century changes of European lead emissions recorded in high-altitude alpine snow and ice. *Environ Sci Technol* 38(4):957–964.
14. Gabrielli P, Cozzi G, Torcini S, Cescon P, Barbante C (2008) Trace elements in winter snow of the Dolomites (Italy): A statistical study of natural and anthropogenic contributions. *Chemosphere* 72(10):1504–1509.

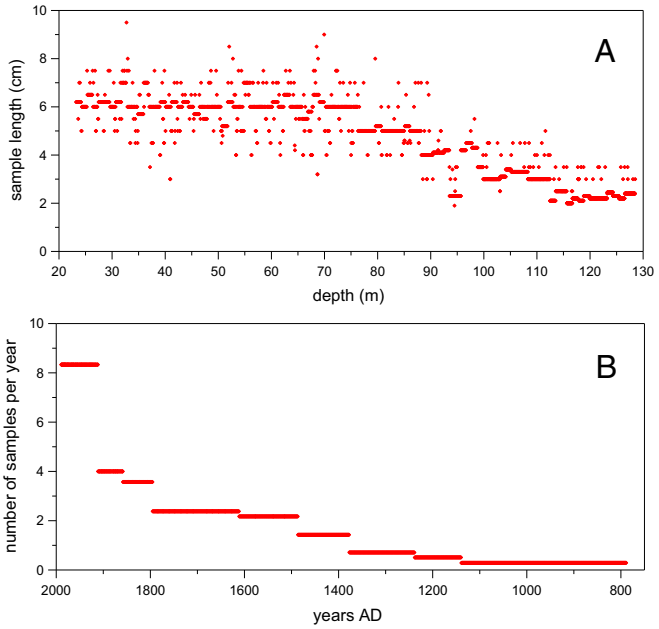

Fig. S1. Spatial resolution adopted for sampling the QND ice core (*A*) and temporal resolution obtained (*B*).

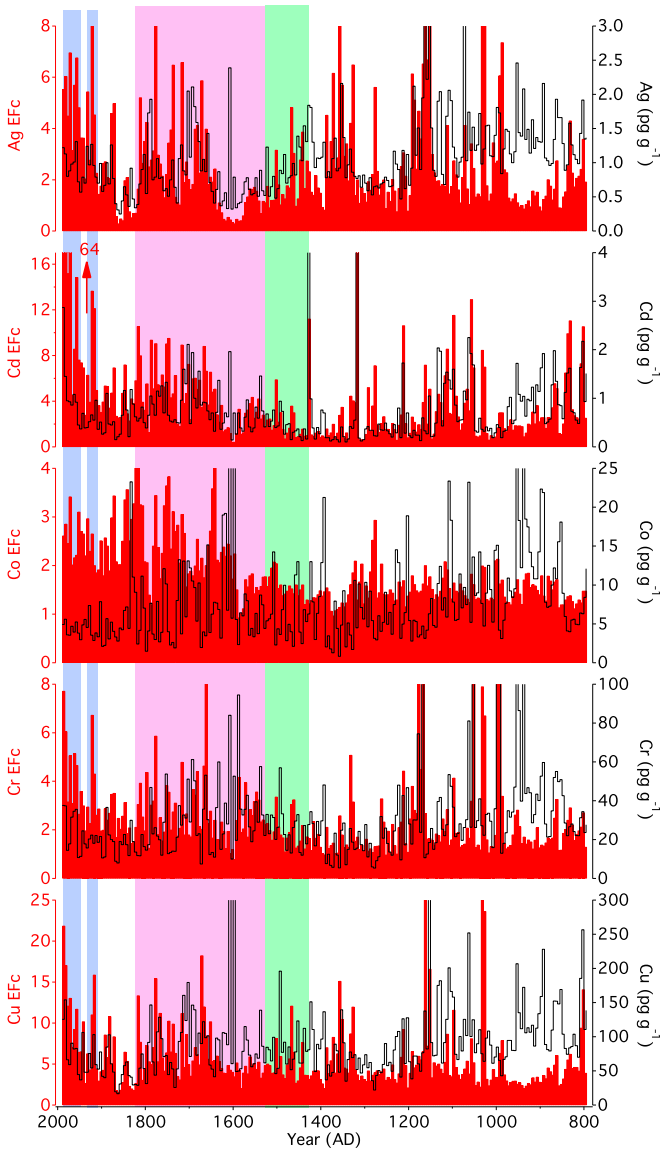

Fig. S2. Five-year median concentrations and crustal enrichment factors (EFc) in QND for Ag, Cd, Co, Cr, and Cu. Colored bands define different historical time periods from A.D. 1438 to A.D. 1532 (Inca Empire; in green) and from A.D. 1532 to A.D. 1833 (Spanish Vice Royalty; in purple). Blue bands highlight the two phases of trace element enrichments during the early and late 20th century.

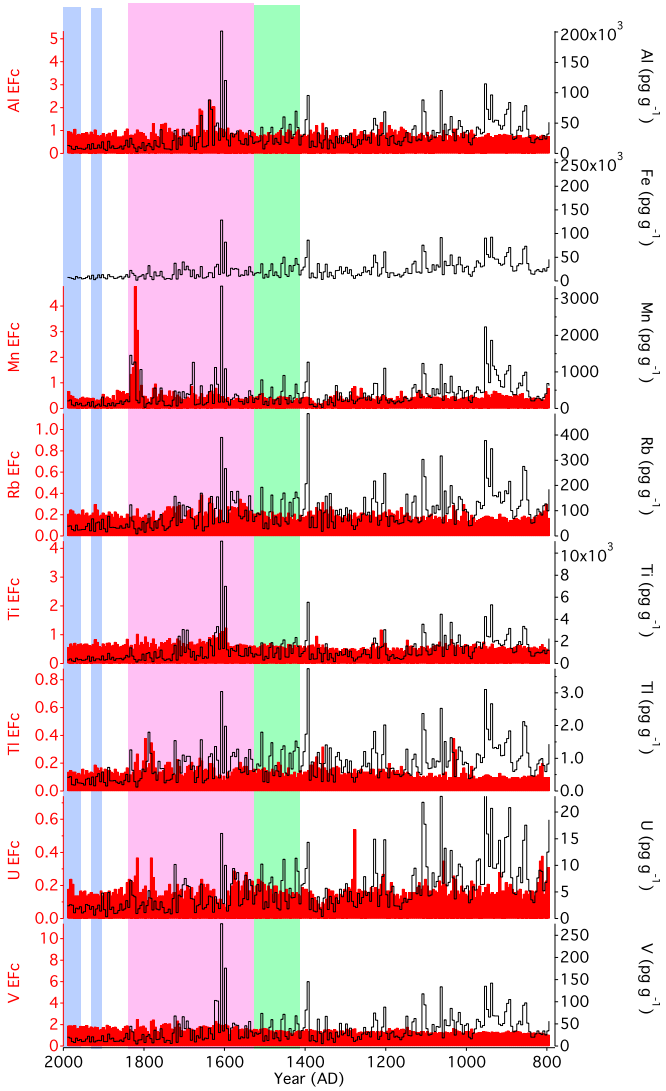

Fig. S3. Five-year median concentrations and EFc in QND for Al, Fe (crustal standard element; only Fe concentrations are displayed), Mn, Rb, Ti, Tl, U, and V. Colored bands define different historical time periods from A.D. 1438 to A.D. 1532 (Inca Empire; in green) and from A.D. 1532 to A.D. 1833 (Spanish Vice Royalty; in purple). Blue bands are reported here only for comparison, as they highlight the two phases of enrichment for most of the trace elements reported in Fig. 2 and Fig. S2 only during the early and late 20th century.

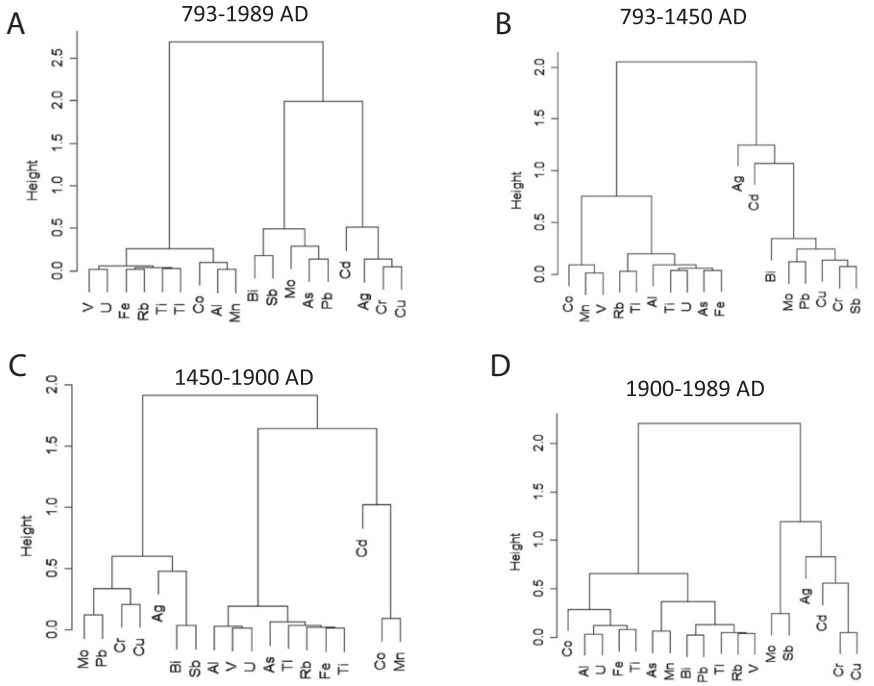

Fig. S4. Dendrograms extracted from the first three principal components of the entire trace element data set (*A*: A.D. 793–1989) and during three subperiods (*B*: A.D. 793–1450; *C*: A.D. 1450–1900; and *D*: A.D. 1900–1989).

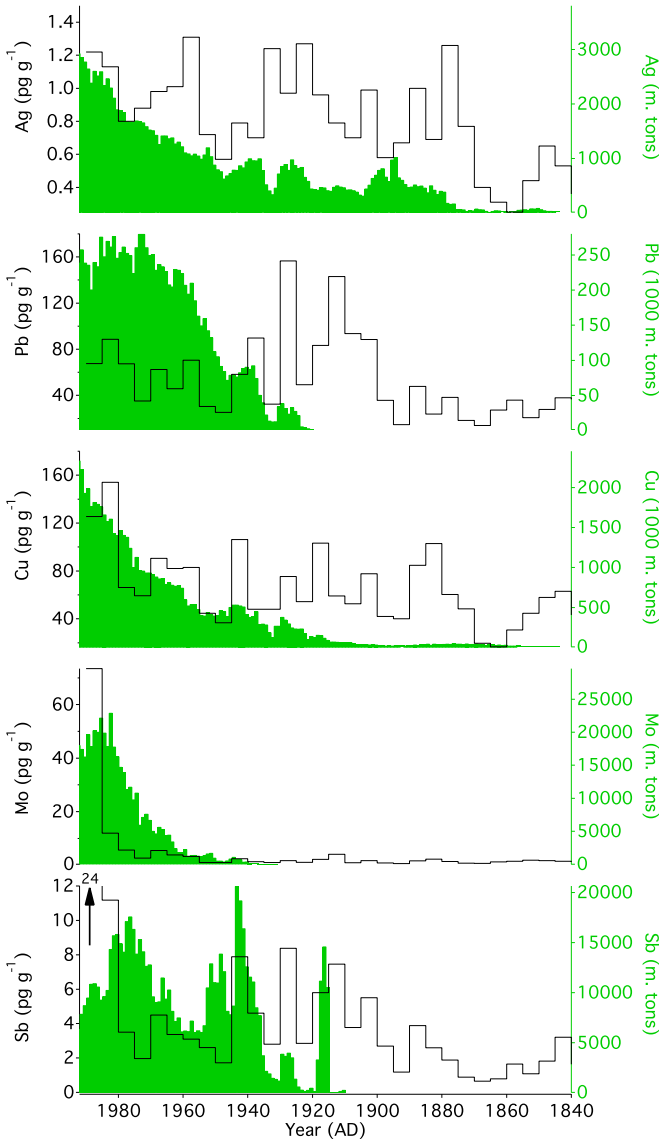

Fig. S5. Five-year median concentrations of Ag, Pb, Cu, Mo, and Sb in QND compared with available corresponding trends in total ore production in South America back to A.D. 1840 (1).

1. Mitchell BR (1998) *International Historical Statistics: The Americas, 1750–1993* (MacMillan, London) 4th Ed.

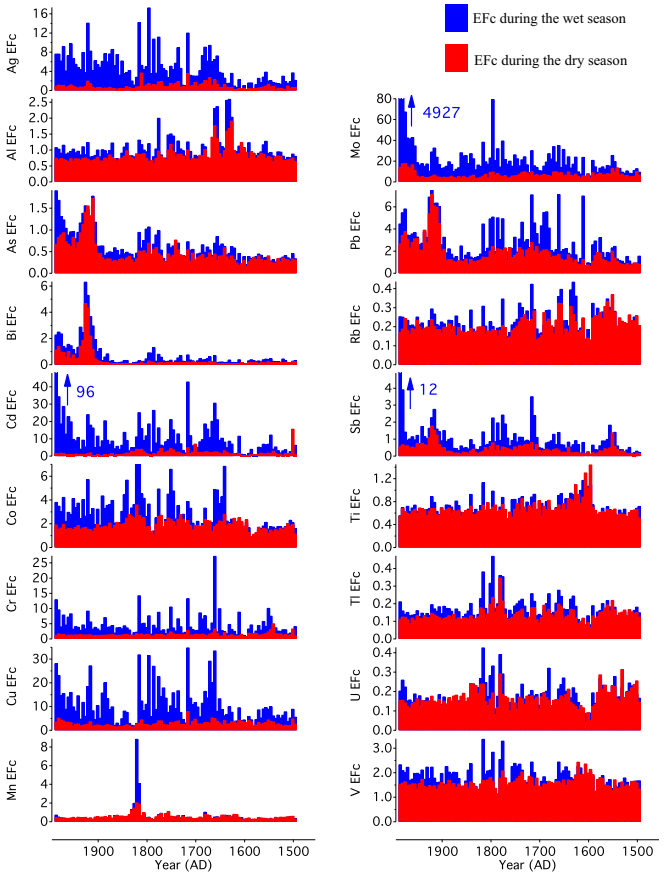

Fig. S6. Five-year median crustal EFc during the dry season and the wet season during the A.D. 1495–1989 time period.

Dataset S1. Median trace element concentrations, fluxes, enrichment factors (EFc), and EFc increase factors during the three examined subperiods. Median concentrations and EFc are calculated as median of the individual sample values. Median fluxes are calculated as median of annual fluxes that are obtained by using annual accumulation and average annual concentrations

Dataset S1

Dataset S2. Trace element composition (as ratios of trace elements and Fe concentrations) of dust collected in the vicinity of the Quelccaya ice cap, Huaynaputina ash in the A.D. 1600 QND ice layers, and Huaynaputina ash in Cerro Trapiche sediments. The crustal EFc in the A.D. 1600 QND ice is then calculated with respect to the elemental composition of Huaynaputina ash from Cerro Trapiche sediments and dust collected near the Quelccaya ice cap

Dataset S2

Dataset S3. Anomalous EFc values recorded in the QND ice core before A.D. 1900. Anomalous EFc values reported in red exceed 3 times and 5 times the median during the A.D. 993–1450 and A.D. 1450–1900 time periods, respectively (see *SI Text*). The ages of the selected ice layers are tentatively matched with possible corresponding volcanic events recorded in Antarctic ice (5)

Dataset S3